TEXTURAL AND CRYSTAL-CHEMICAL EVOLUTION OF A MORB MELT COOLED AT VARIABLE RATES

LETIZIA GIULIANI
Dipartimento di Ingegneria e Geologia (InGeo), Università "G. D'Annunzio" di Chieti-Pescara, Via dei Vestini, 31, 66100, Chieti

The solidification behavior of magmas (melt ± crystals ± dissolved/exsolved volatiles) and lavas strongly depends on magma composition (*X*), *T*, and *P*. Magmas crystallize between *liquidus* (T_m) and *solidus* (T_s) temperatures if kinetics are moderate to low. Conversely, high kinetic conditions induce magmas to solidify at the glass transition temperature (T_g) as glasses. All these thermal parameters vary as a function of X, fO_2, and H_2O, determining also density (ρ), viscosity (η), and ascent velocity (v) of magmas. These physical parameters are nowadays well constrained by thermodynamic models, but effects of variations of *T* and *P* trough time (*t*), *i.e.*, $\Delta T/\Delta t$ and/or $\Delta P/\Delta t$, are still qualitative, albeit their paramount importance. Indeed, solidification rates exert primary control on the evolution of magmas in volcanic domains. Textural and crystal-chemical features of minerals are profoundly dependent on kinetics and, therefore, they can be used to retrieve the crystallization paths of volcanic rocks.

A first analysis was conducted to defines the kinetic and thermodynamic regimes governing the possible ascent, depressurization, and cooling paths, either at intra- and extra-telluric conditions. Finite elements 2D conductive cooling models have been adopted to retrieve the orders of magnitude of ΔT/Δt governing the solidifications of sills, dikes and lava flows with basaltic and rhyolitic compositions, different shapes, volumes, and thermodynamic conditions (*i.e.*, T, Cp, K, α, ρ).

Numerical outcomes show that shallow sills and dikes intruded at few km of depth solidify with $\Delta T/\Delta t$ from 10^{-2} to 10^{-6} °C/h, while in subaerial environments, lava flows up to 2 m of thickness experience $\Delta T/\Delta t$ from 10^3 to ≤ 10^0 °C/h. The outcomes obtained from the simulations suggest that, to fully and quantitatively understand the overall solidification processes of basalts, the thermal ranges of cooling (ΔTc) must be between *liquidus* and *solidus* and $\Delta T/\Delta t$ must systematically change from slow (10^0 °C/h) to fast (10^3 °C/h) conditions. Although there is a lot of experimental study about the solidification of basalts (*e.g.*, Mollo & Hammer, 2017 for a general review), most of them were quenched above T_s, and/or explore only moderate to fast $\Delta T/\Delta t$.

In this work, we focus on the Mid-Ocean Ridge Basalts (MORB), which are the most abundant volcanic products on the Earth's surface. Generally, MORBs have a tholeiitic composition (SiO_2 ~ 50 wt.%, $Na_2O + K_2O$ < 3 wt.%) and contain H_2O ≤ 0.1-0.2 wt.% (Rogers, 2015; Soule, 2015; Wallace *et al.*, 2015). The bulk chemical system investigated in this work corresponds to an Icelandic MORB (USGS standard BIR-1A), labeled B_{100}. The experimental charges were solidified in a ΔTc between 1300°C (*superliquidus*) and 800°C (*solidus*), at *P* and fO_2 of air, using $\Delta T/\Delta t$ of 1, 7, 60, 180, 1800, and 9000 °C/h (Vetere *et al.*, 2013, 2015). The solidified run products were analyzed by SEM-EDS and EMPA-WDS analysis, acquiring several hundreds of back-scattered electron (BSE) SEM images at different magnifications (150 to 3000 X), hundreds of single chemical point analysis, plus tens of chemical profiles on the largest crystals.

The main solidified phases were plagioclase (plg), clinopyroxene (cpx), spinel (sp), and glass. The image analysis was used to quantify the crystal content (area%), 2D crystal size (μm) and shapes, and the number of crystal per area (#/A). At 60 °C/h < $\Delta T/\Delta t$ < 180 °C/h, plg disappeared and cpx and sp shapes changed from faceted to dendritic. In particular, the total crystal content was ~ 100 area% at $\Delta T/\Delta t$ ≤ 60 °C/h, then it decreased to < 2 area% up to 9000 °C/h. Plg abundance monotonically decreased, whereas the cpx content followed an antisymmetric Gaussian trend, increasing from 1 to 180 °C/h and then decreasing up to 9000 °C/h. Sp was present in all the run products, with a constant amount < 5 area%.

The increasing of $\Delta T/\Delta t$ caused the decreasing of the 2D crystal size ranges from 1000-10 to 100-1 μm for plg, from 400-8 to 25-0.5 μm for cpx, and from 90-6 to 6-0.5 μm for sp. The #/A of all phases generally increased up to two orders of magnitudes as the $\Delta T/\Delta t$ increased, except for cpx between 60 and 180 °C/h.

Basing on the 2D textural measurements, the Crystal Size Distribution (CSD) and growth rates (*Gs*) were determined. CSDs increased their slope (*m*) and nucleation density per size (n_0) and showed a general decreasing of the crystal size ranges as the $\Delta T/\Delta t$ increased. Moreover, CSDs of plg, cpx, and sp changed from almost two log-linear segments with different slopes at sluggish $\Delta T/\Delta t$, to a single linear trend at faster $\Delta T/\Delta t$. These features are indicative of different nucleation pulses and growth by coarsening at slow kinetic conditions. Both *m* and n_0 are linearly related with $\Delta T/\Delta t$, allowing to quantitative retrieve the kinetic solidification conditions starting from a simple CSD analysis. The maximum (G_{max}) and average (G_{CSD}) crystal growth rates were calculated using the maximum length (L_{max}) of the 5 longest crystals and the CSDs-*m*, respectively. Both the *G*s are a function of the experimental time, *t*, and increase up to two orders of magnitude with the increasing of $\Delta T/\Delta t$. Moreover, the G_{max} of cpx is linearly related to *m* and n_0 of the cpx-CSD. In turn, the CSD of cpx hosted in MORBs can quantify their growth rates.

Importantly, plg and cpx crystals with sizes between 0.1 and 1 mm can grow at $\Delta T/\Delta t$ conditions (1 and 7 °C/h) typical of the innermost part of lava flows with thickness ≥ 1 m. In turn, mm-sized crystals are not invariably indicative of deep processes but can grow in *syn*-to *post*-eruption conditions.

The mineral chemistry of the plg, cpx, and sp solidified in the B_{100} run products were quantified by measuring the major oxides elements (wt.%), and by calculating the cation abundances (a.p.f.u.) and molecular components. Crystal-chemical results showed that variations into plg were limited, whereas cpx and partially sp well recorded cooling dynamics. The residual glass (≤ 50 μm from the crystal rim) obtained at 180-1800 °C/h showed compositional variations related to the surrounding crystal growth, evidencing strong supersaturation phenomena due to the establishment of a diffusion-controlled growth regime.

In particular, Mag (magnetite), Sp *s.s.* (spinel *sensu stricto*) and Usp (ulvospinel) end-members changed of < 10 mol.% when $\Delta T/\Delta t$ shifts from 1 to 9000 °C/h. Cpx were mainly composed of Di (diopside) + En (enstatite), although the CaTs (Ca-tschermak) became significative at higher $\Delta T/\Delta t$. Ab (albite) and An (anorthite) contents in plg poorly changed, maintaining an average molecular formula of $An_{70}Ab_{30}$. However, Fe_2O_3 in sp, CaO, Fe^{2+}, $Fe^{3+,}$ and Ca in cpx and SiO_2, Al_2O_3, Fe_2O_3 and MgO, Si, Al, and Fe^{3+} in plg were linearly related with the $\Delta T/\Delta t$ variations and represent geospeedometers. In the same manner, Fe^{2+}/Fe^{tot} and Mg# in cpx, as well as Mag, Fs, and CaFeTs were highly linearly related to $\Delta T/\Delta t$. Cation variations into cpx, as well as their most abundant or linearly related molecules, were also related to each other, showing high linear correlations.

The mineral chemistry of sp, cpx, and plg was related to the computed G_{max} and G_{CSD}, founding quantitative linear relationships between these textural parameters and some oxides and molecular components.

The analytical relationships between textural-chemical features and cooling kinetics made possible to carefully reconstruct the solidification conditions of MORB melts. Moreover, the chemistry of cpx and plg was used to attest the *equilibrium* or *disequilibrium* crystallization conditions. Particularly, cpx compared with bulk composition suggested the attainment of near-*equilibrium* crystallization conditions at $\Delta T/\Delta t \leq 60$ °C/h, whereas *disequilibrium* effects were found at $\Delta T/\Delta t > 60$ °C/h. In contrast, plg was systematically in *disequilibrium* with the MORB melt and its crystallization took place at lower *T* than cpx. These results, coupled with the textural analysis, suggested the switching between an interface-controlled mechanism at $\Delta T/\Delta t \leq 60$ °C/h and a diffusion-controlled growth mechanism for faster $\Delta T/\Delta t$ conditions.

Once quantified the texture and mineral chemistry of the B_{100} MORB composition, to further investigate the solidification processes, the same starting material was investigated by *in-situ* differential scanning calorimetry (DSC). This technique is a proxy to investigate the solidification processes in the Material Science, but it is very rarely applied for the more chemically complex systems in the Earth Science (Onorato *et al.*, 1980; Ray *et al.*, 2005; Iezzi *et al.*, 2017). In particular, the DSC experiments were run following similar solidification paths of the previous *ex-situ* experiments, *i.e.* ΔTc between 1300°C (*superliquidus*) and 800/600°C (*solidus*), *P*

and fO_2 of air, and $\Delta T/\Delta t$ of 7, 60, 180, 1000 and 1800 °C/h. As for the *ex-situ* experimental charges, also these new run products were analyzed by SEM-EDS to acquire BSE-images at different magnifications (150-1000x).

The solidified phases in all the run products were glass, cpx, sp, and melilite (mel), whereas plg was present only at 7 °C/h with an amount < 2 area%. The cpx and sp contents were comparable with those measured from the *ex-situ* experimental charges, and mel was always ≤ 10 area%. The total crystal content slightly increased from 7 to 1800 °C/h, mirroring the same trend measured for the *ex-situ* run product in this $\Delta T/\Delta t$ range. CSDs analysis for both cpx and sp showed that trends at 7 and 60 °C/h were composed of at least two log-linear segments with different slopes. Also in this case, this feature is related to different pulses of crystal nucleation, followed by crystal growth by coarsening. The Gmax and GCSD were computed using the time ranges directly measured *in-situ*, representing the most accurate and reliable estimates obtained for MORBs. Hence, when $\Delta T/\Delta t$ increased both the Gs of cpx and sp increased as well.

The *in-situ* acquisition of the DSC spectra allowed to directly measure the crystallization steps, in terms of T_m, T_g, and T_x (onset of the crystallization). In particular, T_m and T_g were measured during heating, whereas T_x peaks were identified both on heating and on cooling. Values of T_m and T_g corresponded to 1206 (±1)°C and 698 (±3)°C, respectively, resembling those computed by Vetere *et al.* (2015) (*i.e.*, T_m = 1233°C and T_g = 651°C). T_x estimations allowed defining a maximum thermal range of crystallization between 911 (±65)°C and 1126 (±36)°C. The DSC *in-situ* experiments from 7 to 1800 °C/h confirmed that sp was the first phased to nucleate, followed by cpx and mel (or plg). T_x measured along the cooling paths (T_{x_CR}) showed high-T exothermic peaks that change from a single symmetric shape (7 and 60 °C/h) to multi-component patterns (180, 1000, and 1800 °C/h). The temperature of the onset of crystallization on cooling (T_{xi}) was measured at 10% of the maximum intensity of the DSC crystallization peak on cooling. It progressively decreased as the $\Delta T/\Delta t$ increased, following an exponential trend. This latter was used to retrieve the values of T_{xi} for different ΔT/Δt conditions. This T_{xi} trend mirrored the uppermost portion of a time-transformation-temperature (TTT) curve.

All the obtained outcomes in this work refer to the widest dynamic experimental range investigated in the Earth Sciences and can be used to define quantitative solidification models of dry basaltic melts (Fig. 1). This enlarges the previous investigations and furnishes a more reliable and quantitative picture of the solidification behavior of dry MORBs. A practical demonstration of this is shown in two quantitative models exposing the section of MORB lava flows with 0.5 and 1.5 m of thickness. These models allow to retrieve the kinetic conditions of crystallization from textural parameters (*e.g.* area%, #/A, CSD, L_{max} and *G*s) and/or from simple EPMA analysis (*e.g.*, CaO for cpx, Al_2O_3 for plg and Fe_2O_3 for sp) as well as for chemical component (*e.g.*, Di/(En + CaTs), and Mag).

The $\Delta T/\Delta t$ governing the solidification of lava flows were deduced from the numerical modeling exposed in Giuliani *et al.* (2020a; 2020b) and are on the order of $10^1/10^0$ °C/h in the innermost parts and of 10^3 °C/h in their outermost portions. For both the modeled MORB lava sections, the glass amount decreased from 44 area% to ≤ 5 area%, leading to holocrystalline products in the innermost areas. The #/A (μm^{-2}) followed a parabolic trend, decreasing from 10^{-1} to $10^{-3}/10^{-4}$ μm^{-2} towards the innermost part and then increasing again up to $10^{-2}/10^{-1}$ μm^{-2} at the bottom of the lava flow. The CSDs variations were shown only for cpx, the most representative, and abundant crystalline phase. In the innermost portion of the 1.5 m thick lava flow, the log-linear segments of CSDs at the center of the flow (slowest $\Delta T/\Delta t$) reflected multiple nucleation events, followed by growth mechanisms by coarsening. Crystals had their maximum lengths in the sluggish cooled portions of lava flows, the spacing between few μm up to 250 and 750 μm for cpx and plg in the 0.5 m thick flow, and up to 500 and 1000 μm in the 1.5 m thick lava flow.

These outcomes have important petrological implications, suggesting that plg and cpx crystals with sizes of 10^2 to 10^3 μm may also develop after the eruption from anhydrous MORB lava flows and pillows. Thereby, crystal sizes, considered to represent phenocrysts and microphenocrysts, are not unequivocally indicative of crystal growth in magmatic reservoirs or conduits.

Crystal growth is slower in the center of the lava flow and increase of more than one order of magnitude moving toward the top of the flow. In MORB lava flows with a thickness of both 0.5 and 1.5 m, the crystallization will start at less than 1000°C in the shallowest portions, whereas in the inner of the flow it will occur at around 1125°C.

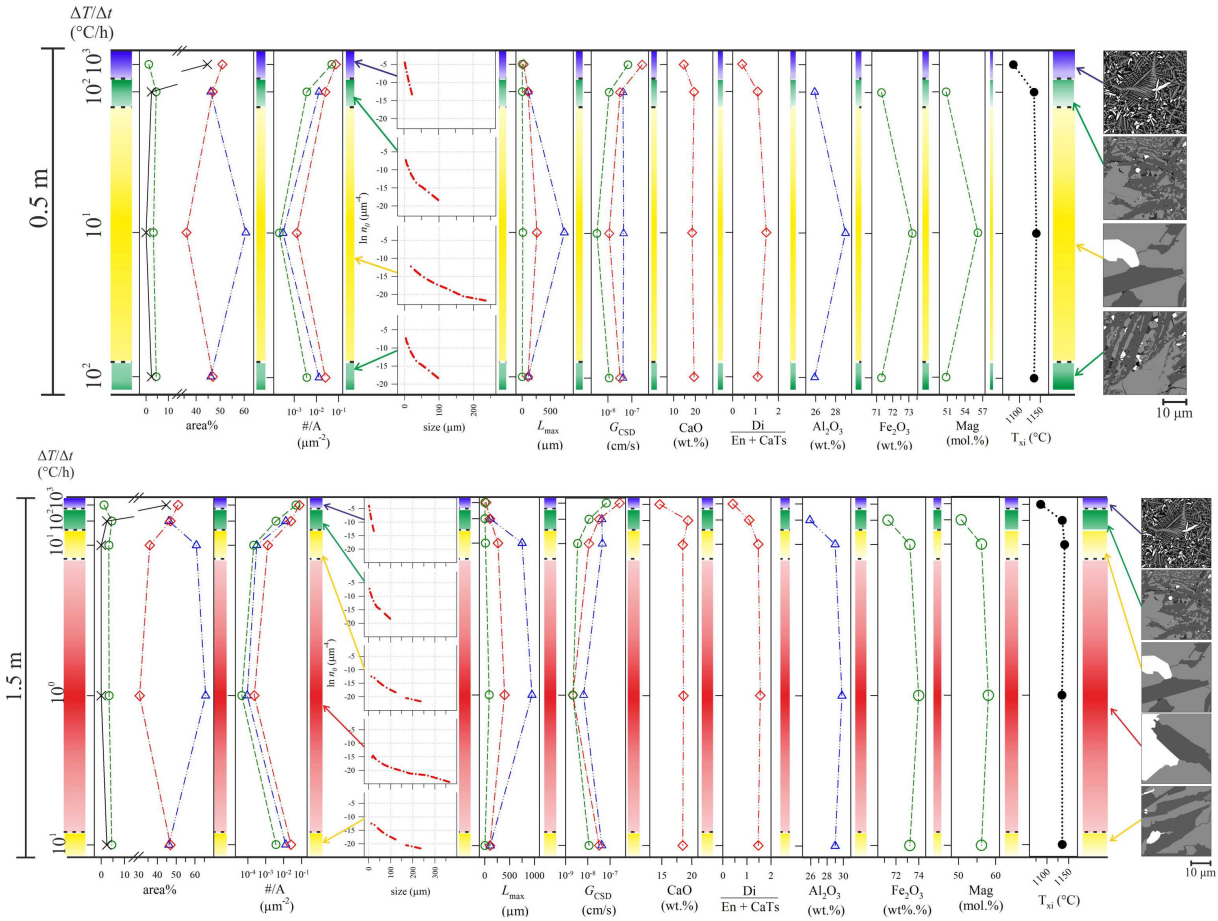

Fig. 1 - Hypothetical solidification sketch of a MORB lava with a thickness of 0.5 m (top) and 1.5 m (bottom). ΔT/Δt (°C/h) and textural parameters are those measured by Giuliani *et al.* (2020a, 2020b). Qualitative textures on the right side of the figure are modified from the experiments of Vetere *et al.* (2013, 2015).

REFERENCES

Giuliani, L., Iezzi, G., Mollo, S. (2020a): Dynamics of volcanic systems: physical and chemical models applied to *equilibrium versus disequilibrium* solidification of magmas. *In*: "Dynamic Magma Evolution", F. Vetere ed., Geophysical Monograph Series, American Geophysical Union., John Wiley & Sons, Inc., 100-122.

Giuliani, L., Iezzi, G., Vetere, F., Behrens, H., Mollo, S., Cauti, F., Ventura, G., Scarlato, P. (2020b): Evolution of textures, crystal size distributions and growth rates of plagioclase, clinopyroxene and spinel solidified at variable cooling rates from a mid-ocean ridge basaltic liquid. *Earth-Sci. Rev.*, **204**, 103165.

Iezzi, G., Elbrecht, A.L., Davis, M., Vetere, F., Misiti, V., Mollo, S., Cavallo, A. (2017): Glass Stability (GS) of chemically complex (natural) sub-alkaline glasses. *J. Non-Cryst. Solids.*, **477**, 21-30.

Mollo, S. & Hammer, J.E. (2017): Dynamic crystallization in magmas. *In*: "Mineral reaction kinetics: microstructures, textures, chemical and isotopic signatures", W. Heinrich & R. Abart, eds. *EMU Notes in Mineralogy,* European Mineralogical Union and the Mineralogical Society of Great Britain & Ireland, **16**, 1-46.

Onorato, P.I.K., Uhlmann, D.R., Hopper, R.W. (1980): A kinetic treatment of glass formation: IV. Crystallization on reheating a glass. *J. Non-Cryst. Solids.*, **41**, 189-200.

Ray, C.S., Reis, S.T., Brow, R.K., Höland, W., Rheinberger, V. (2005): A new DTA method for measuring critical cooling rate for glass formation. *J. Non-Cryst. Solids*., **351**, 1350-1358.

Rogers, N. (2015): The composition and origin of magmas. *In*: "The encyclopedia of volcanoes, 2nd edition", H. Sigurdsson, B. Houghton, S.R. McNutt, H. Rymer, J. Stix, eds. Elsevier Inc., 93-112.

Soule, S.A. (2015): Mid-Ocean Ridge Volcanism. *In*: "The encyclopedia of volcanoes, 2nd edition", H. Sigurdsson, B. Houghton, S.R. McNutt, H. Rymer, J. Stix, eds. Elsevier Inc., 395-403.

Vetere, F., Iezzi, G., Behrens, H., Cavallo, A., Misiti, V., Dietrich, M., Knipping, J., Ventura, G., Mollo, S. (2013): Intrinsic solidification behavior of basaltic to rhyolitic melts: a cooling rate experimental study. *Chem. Geol*., **354**, 233-242.

Vetere, F., Iezzi, G., Behrens, H., Holtz, F., Ventura, G., Misiti, V., Cavallo, A., Mollo, S., Detrich, M. (2015): Glass forming ability and crystallization behavior of sub-alkaline silicate melts. *Earth-Sci. Rev*., **150**, 25-44.

Wallace, P.J., Plank, T., Edmonds, M., Hauri, E.H. (2015): Volatiles in Magmas. *In*: "The encyclopedia of volcanoes, 2nd edition", H. Sigurdsson, B. Houghton, S.R. McNutt, H. Rymer, J. Stix, eds. Elsevier Inc., 163-183.